

# Optical tweezers with cylindrical vector beams produced by optical fibers

Giovanni Volpe<sup>a</sup>, Gajendra P. Singh<sup>a</sup>, and Dmitri Petrov<sup>a,b</sup>

<sup>a</sup>Institut de Ciències Fotòniques (ICFO), Barcelona, Spain

<sup>b</sup>Institució Catalana de Recerca i Estudis Avançat (ICREA), Barcelona, Spain

## ABSTRACT

Gradient radiation forces exerted by strongly focused cylindrical vector beams of radial and azimuthal polarizations on dielectric spheres of different radii and refractive indices were calculated. The effect of longitudinal and transversal components of the focused electrical field on trapping properties was studied. Experiments on optical trapping were performed using low-mode optical fiber excited with Laguerre-Gaussian beam as a source of the trapping beams.

**Keywords:** optical tweezers, optical fibre, cylindrical vector beam, polarization, Laguerre-Gaussian mode

## 1. INTRODUCTION

The trapping of nano- and micro-particles by using the radiation forces produced by highly focused optical beams (so-called optical tweezers) has become very widely used in the past two decades in physical, chemical, and biological experiments where precise manipulation of microscopic objects is required. The scattering and gradient optical forces exerted on the trapped objects depend on the intensity and phase distributions in a trapping beam. For this reason optical trapping has been studied for different types of optical beams, for example, Gaussian, Laguerre-Gaussian, Bessel.<sup>1</sup>

One promising type of beams for optical trapping is Bessel-Gaussian vector beam, that are solutions of the vector wave equation in the paraxial limit.<sup>2,3</sup> Some of these solutions obey cylindrical symmetry both in amplitude and polarization, hence the name cylindrical vector beams, CVB.

The peculiar features of CVB have attracted a great deal of interest from researchers. Possible applications include, for example, focusing of atoms,<sup>4</sup> material processing,<sup>5</sup> microellipsometry,<sup>6</sup> and spectroscopy.<sup>7</sup> For optical trapping the most interesting features arise from the focusing properties of these beams.<sup>8,9</sup> In particular, a radially polarized CVB focused by a high numerical aperture objective has a peak at the focus, and an azimuthally polarized incident beam has a null in the center. Switching between radial and azimuthal polarizations can be done by using two half-wave plates. The radiation forces on dielectric spheres produced by CVB of different polarizations have so far only been calculated in the Rayleigh regime (with a particle radius of 50 nm<sup>10</sup>). No experimental results have been published yet. In this paper we calculate the gradient forces acting on dielectric particles of arbitrary radius using the simplified description proposed in.<sup>11</sup> Experimental results on optical trapping of low- and high-refractive index particles using CVB generated with a few-mode optical fiber are also presented.

## 2. THE GRADIENT TRAPPING FORCES ACTING ON A DIELECTRIC SPHERE IN THE CYLINDRICAL VECTOR BEAM

Figure 1(a) shows the geometry of the problem. The incident field with a known spatial distribution of the electrical field amplitude and polarization has a planar wavefront at the entrance pupil of a lens with numerical aperture  $NA$ . The lens produces a converging, spherical wave which propagates along the axis  $z$  to a axial point

---

Further author information: (Send correspondence to Dmitri Petrov: E-mail: Dmitri.Petrov@icfo.es, Telephone: 34 93 413 7942)

image at the plane  $z = 0$ . The focal field generated by a generalized cylindrical vector beam illumination of the input pupil can be written as<sup>8</sup>:

$$\vec{E}(r, \varphi, z) = E_r \vec{e}_r + E_\varphi \vec{e}_\varphi + E_z \vec{e}_z,$$

where  $\vec{e}_r$ ,  $\vec{e}_\varphi$ , and  $\vec{e}_z$  are the unit vectors in the radial, azimuthal, and  $z$  directions, respectively. The amplitudes of the three orthogonal components are given by

$$\begin{aligned} E_r(r, \varphi, z) &= A \cos \phi \int_0^\alpha \sqrt{\cos \theta} p(\theta) \sin \theta \cos \theta J_1(kr \sin \theta) e^{ikz \cos \theta} d\theta, \\ E_z(r, \varphi, z) &= iA \cos \phi \int_0^\alpha \sqrt{\cos \theta} p(\theta) \sin^2 \theta J_0(kr \sin \theta) e^{ikz \cos \theta} d\theta, \\ E_\varphi(r, \varphi, z) &= A \sin \phi \int_0^\alpha \sqrt{\cos \theta} p(\theta) \sin \theta J_1(kr \sin \theta) e^{ikz \cos \theta} d\theta, \end{aligned}$$

where  $p(\theta)$  is the pupil anodization function,  $k$  is the wave number, and  $J_n$  is the Bessel function of the first kind with order  $n$ ,  $A$  is the amplitude of the field, that is defined by the beam power  $P$ . The beam has a polarization rotated by  $\phi$  from its radial direction. For pupil function we use a Bessel-Gaussian beam at plane  $z = 0$ , where the phase front is assumed to be planar<sup>8</sup>:

$$p(\theta) = \exp[-\beta^2 (\frac{\sin \theta}{\sin \alpha})^2] J_1(2\beta \frac{\sin \theta}{\sin \alpha}),$$

where  $\beta$  is the ratio of the pupil radius and the beam waist,  $\alpha$  is defined by the numerical aperture of an objective and by the refractive index  $n_a$ :  $\alpha = \sin^{-1}(NA/n_a)$ . Here  $n_a$  is the refractive index of the medium.

For calculation of the gradient optical trapping force we use an approximation proposed in<sup>11</sup> for strongly focused beams. This theory fits well with measurements made for particles of different sizes from nanometers to microns. However, the theory can be considered only as an approximation in the full problem of the optical trapping because it neglects the scattering radiation force and that the dielectrics should not be strongly polarized.

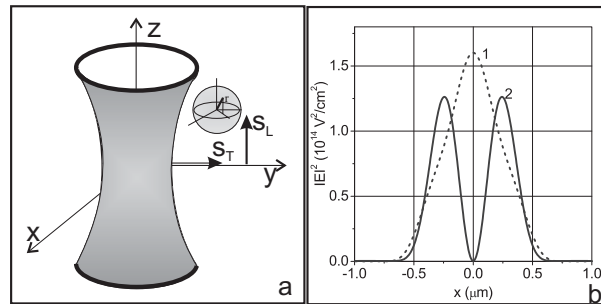


**Figure 1.** a) Geometry of the problem, and b)  $|E|^2$  distribution at the focal plane  $z = 0$  along the  $x$ -axis for radial (1) and azimuthal (2) polarization incident beams focused by an objective with  $NA = 1.3$ .

Following this theory the dipole interaction energy of an dielectric particle in the field of the strongly focused beam is given by

$$W(s) = -\left(\frac{n_p^2}{n_0^2} - 1\right) \int I(s) dV,$$

where  $I$  is the energy density of the optical beam,  $V$  is the volume of the particle, and  $s$  is the distance between the center of the beam and the position of the particle center of mass (see Fig.1a).

The changes of the energy of the particle when it moves in the transverse ( $x$  or  $y$ ) direction can be written as:

$$W_T(s) = -a \int_0^R dr r^2 \int_0^{2\pi} d\varphi \int_0^\pi d\theta \sin \theta \left| \vec{E}(s + r \sin \theta \cos \varphi, r \sin \theta \sin \varphi, r \cos \theta) \right|^2,$$

or in the axial ( $z$ ) direction

$$W_A(s) = -a \int_0^R dr r^2 \int_0^{2\pi} d\varphi \int_0^\pi d\theta \sin \theta \left| \vec{E}(r \sin \theta \cos \varphi, r \sin \theta \sin \varphi, s + r \cos \theta) \right|^2,$$

that give the transverse and axial forces which tend to pull the particle back to its equilibrium center:

$$F_{T,A}(s) = -\frac{\partial W_{T,A}(s)}{\partial s}.$$

Here  $a = \left(\left(\frac{n_p}{n_0}\right)^2 - 1\right) \frac{n_0 \varepsilon_0}{2}$ ,  $\varepsilon_0$  is the vacuum permittivity, and  $R$  is the radius of the particle.

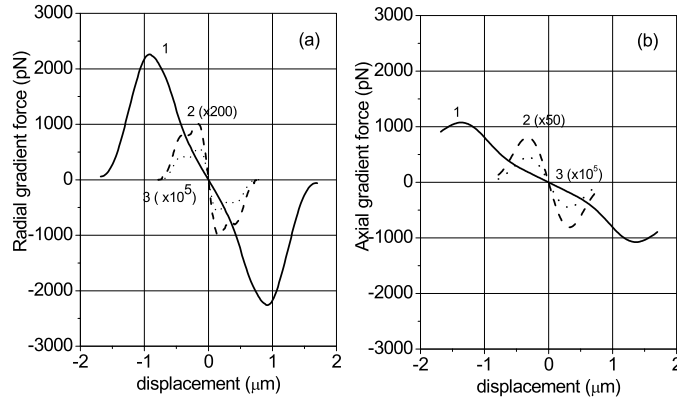


**Figure 2.** Force-displacement curves for the particles of different radii in the field of the radially polarized CVB. a) transversal force and b) axial force.  $R = 1000nm(1)$ ,  $R = 100nm(2)$ ,  $R = 10nm(3)$ .

We calculated numerically the transversal and axial gradient forces versus the displacement assuming the numerical aperture  $NA=1.3$ , the light wavelength  $0.53\mu m$ , the input power  $P = 1W$ , and the refractive indices  $n_a = 1.33$  and  $n_p = 1.55$ . The field distribution at the focal plane of the radial and azimuthal incident beam is shown in Figure 1b and fits well with previously published results.<sup>8, 10</sup> Figure 2 shows the gradient forces for a radially polarized incident beam. As seen, both the transversal and axial forces permit the trapping of high-refractive index particles. However the optical trapping is impossible by gradient forces for low-refractive particles ( $n_p < n_0$ ). Even if we take into consideration the scattering force, this force can compensate only for the axial gradient force and the transversal gradient force would repel the particles from the focal spot.

If the illumination of the focusing lens is azimuthally polarized, (see Figure 3) the axial gradient force permits one to trap high refractive index particles of any size. The interesting property of such a trap is that the force-displacement curve  $F_T(s)$  changes its sign near the equilibrium point when the particle radius grows. Therefore, the transversal gradient force also can trap the high refractive particles with  $R > 500 nm$ , however it cannot trap the particles with  $R < 500 nm$ . The low-refractive particles of such a radius experience a gradient transversal force towards the equilibrium point and subsequently they are repelled from this point by the axial forces. However, the scattering radiation force can compensate this repulsive axial gradient force, as described in,<sup>12</sup> and therefore the azimuthally polarized CVB can trap the low-refractive particles with  $R < 500 nm$ .

The intensity distribution near the focus depends on numerical aperture of the focusing objective. One can expect essential changes of the trapping properties of the same input beam by changing  $NA$ . Especially this should be important for the radial illumination of the input pupil, when the beam consists of the transversal  $E_r$  and longitudinal  $E_z$  orthogonal components. The  $E_z$ -component decreases when  $NA$  increases, while the  $E_r$  does not change essentially. As seen in Figure 4 the low- $NA$  objective produces a doughnut shape of the total intensity distribution, however the high- $NA$  objective produces a peak at the focus. Figure 5 shows the transversal and axial gradient forces acting on a  $500nm$  particle when the input radially polarized CVB is focused by objectives with different  $NA$ .

The radial gradient force traps the high-index particle when the beam is focused by the  $NA = 0.7$  and  $NA = 1$  objectives, while it repels the particle in the radial direction if  $NA = 1.3$ . The axial gradient force permits to achieve a stable trapping of high-index particles for any value of  $NA$ . For low-index particles the scattering force together with the gradient force may provide the stable axial trapping.

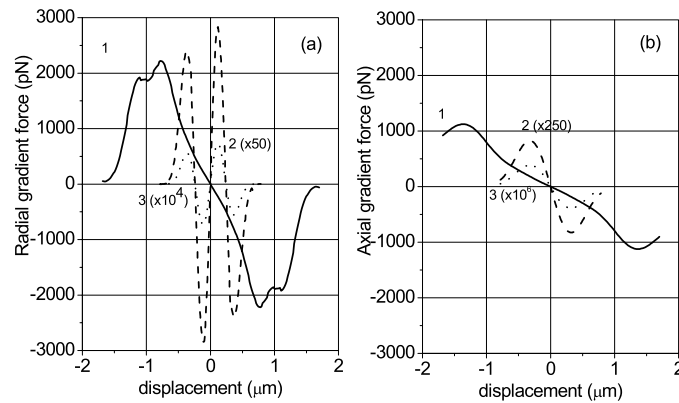


**Figure 3.** Force-displacement curves for the particles of different radii in the field of the azimuthally polarized CVB. a) transversal force and b) axial force.  $R = 1000nm$ (1),  $R = 100nm$ (2),  $R = 10nm$ (3).

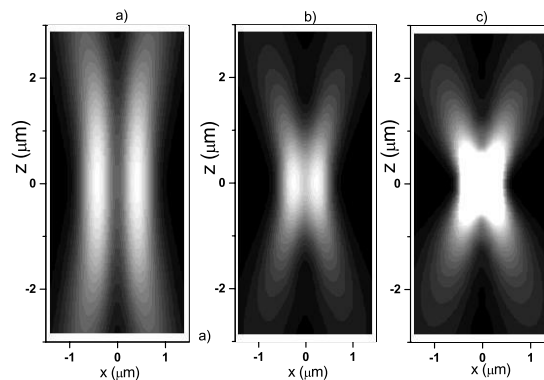


**Figure 4.** Intensity distribution at the  $xz$ -plane produced by the radially polarized CVB pupil illumination focused with the objectives of different  $NA$ .  $NA = 0.7$ (a),  $NA = 1.0$ (b),  $NA = 1.3$ (c).

### 3. GENERATION OF CVB WITH A FEW-MODE FIBER

For experimental realization of the optical trapping with CVB one needs first to generate beams with such kind of polarization. Various alternative methods have been proposed to produce CVB: a double interferometer configuration to convert a linearly polarized laser beam into a radially polarized one<sup>13</sup>; the summation inside a laser resonator of two orthogonally polarized  $TEM_{01}$  modes<sup>14</sup>; computer-generated sub-wavelength dielectric gratings<sup>15</sup>; a space variant liquid crystal cell<sup>16</sup>; a radial analyzer consisting of a birefringent lens<sup>6</sup>; a surface-emitting semiconductor laser<sup>17</sup>; an excitation of a few-mode optical fiber with an offset linearly polarized Gaussian beam.<sup>18</sup> In this paper we use a novel technique to generate CVB.<sup>19</sup>

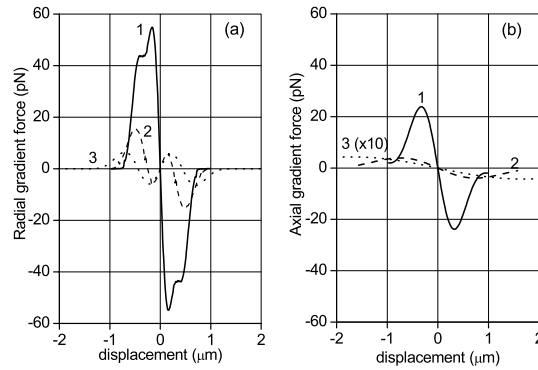


**Figure 5.** Force-displacement curves for the 500nm particle in the field of the radially polarized CVB focused by the objectives of different NA. a) transversal force and b) axial force.  $NA = 0.7(1)$ ,  $NA = 1.0(2)$ ,  $NA = 1.3(3)$ .

The main idea of this technique is as follows. Along with the fundamental mode  $LP_{01}$  ( $HE_{11}$ ), the few-mode fiber supports also the modes  $LP_{11}$  ( $TE_{01}$ ,  $TM_{01}$ , and  $HE_{21}$ ).<sup>20</sup> These modes are reminiscent of CVB. In particular, the modes  $TE_{01}$  and  $TM_{01}$  present, respectively, an azimuthally and radially polarized electric field, while the mode  $HE_{21}$  has a hybrid structure. To excite preferably a mode from the group  $LP_{11}$  one can distribute the input power in a doughnut shape, for example, using a first order Laguerre-Gaussian  $LG_{1,0}$  beam at the input of the fiber instead of a Gaussian beam. The propagation constants of the  $LP_{11}$  modes are different; hence the polarization state of the total field varies along the fiber. When the light reaches the fiber output, it excites a Bessel-Gaussian beam in free-space.<sup>2,3</sup> This special kind of beams preserves the main polarization features that characterize the fiber modal fields. In particular, some of these beams present a cylindrically symmetrical polarization.

Usually a combination of  $LP_{11}$  modes is excited. For this reason the Bessel-Gaussian beam in free-space does not necessarily have a cylindrically symmetrical polarization. However it is possible to obtain any kind of CVB with a pure polarization rotator consisting of two half-wave plates.<sup>6</sup>

Let us first calculate the coupling coefficients between an input  $LG_{1,0}$  beam and the  $LP_{11}$  modes of a few-mode step-index optical fiber. As an example, we assume that a core radius  $a_{co} = 2.15 \mu m$  and a refractive index height profile parameter<sup>20</sup>  $\Delta = 0.34\%$ . The wavelength is assumed to be  $\lambda = 632.8 nm$ . These are the parameters of the commercial fiber used in our experiments (Thorlabs, FS-SN-4224).

If the waist of the input beam is placed at the fiber input at  $z = 0$ , the electric field is given by:

$$\mathbf{E}_i(r, \phi) = \mathbf{A} \frac{r}{w_0} e^{-\frac{r^2}{w_0^2}} e^{i\phi}, \quad (1)$$

where  $\mathbf{A}$  is a constant that defines the polarization and amplitude of the beam,  $w_0$  is the beam waist,  $r$  and  $\phi$  are the radial and azimuthal coordinates, respectively.

With the total electric field  $\mathbf{E}_t$  at the fiber input known, the amplitudes of the excited modes can be calculated through<sup>20</sup>:

$$a_j = \frac{1}{2N_j} \int_{A_\infty} \mathbf{E}_t \times \mathbf{h}_{tj}^* \cdot \hat{\mathbf{z}} dA, \quad (2)$$

where  $\mathbf{h}_{tj}^*$  is the transverse component of the magnetic field of the  $j^{th}$  mode,  $A_\infty$  is the infinite cross section,  $N_j$  is a normalization factor, and  $\hat{\mathbf{z}}$  is the unit vector along the propagation direction.

The power  $P_j$  of the  $j^{th}$  mode is given by:

$$P_j = \frac{|a_j|^2 N_j}{P_T}, \quad (3)$$

where  $P_T$  is the input beam power.

Using Eqs. (1) through (3) and the expression of the modal fields given in,<sup>20</sup> we found numerically the coupling coefficients for an input  $LG_{1,0}$  beam with different waists  $w_0$ . The beam was always considered to be centered on the fiber with neither tilt nor offset.

If the input beam has a circular polarization  $+\sigma$ , so that the rotation directions of the phase and polarization coincide, the  $TE_{01}$  and  $TM_{01}$  modes are excited with the same efficiency (Fig. 6a). At the optimum size of the waist,  $w_{opt} \cong 1.9a_{co}$ , 56% of the total power is coupled to these modes; the rest is transmitted by radiation modes. The power coupled into the fundamental mode  $LP_{01}$  and  $HE_{21}$  modes is negligible. When the waist is increased beyond the optimum value the coupled power decreases slowly. The modal amplitude phases vary significantly, but with a constant difference of  $\pi/2$  between the  $TE_{01}$  and  $TM_{01}$  modes (Fig. 6b).

The same considerations can be stated when the input beam has a circular polarization  $-\sigma$ , so that the polarization and phase of the input beam rotate in opposite directions. The main difference is that only the even and odd  $HE_{21}$  modes are excited. Hence, the phase singularity in the input beam causes the  $+\sigma$  and  $-\sigma$  excitations to be different, and permits to excite selectively different sets of modes from the  $LP_{11}$  group.

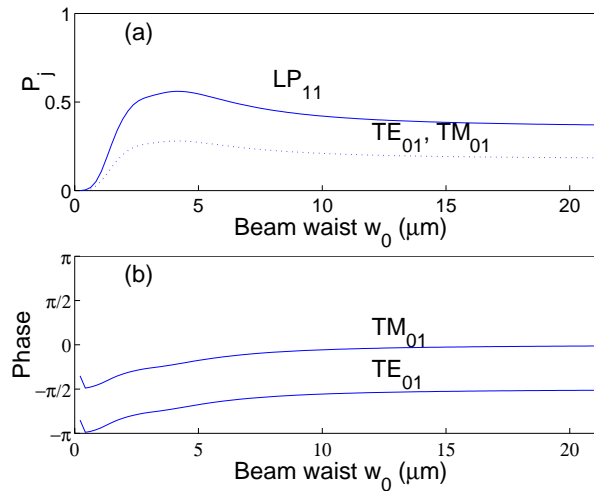


**Figure 6.** Excitation with a  $+\sigma$  beam for different input beam waist. (a) Total power coupled into the modes of the  $LP_{11}$  group (solid line). The dotted line plots the power coupled into each of the modes  $TE_{01}$  and  $TM_{01}$ . (b) Phases of the excited  $TE_{01}$  and  $TM_{01}$  modes at the input.

The state of total field polarization varies along the fiber because there are three propagation constants for these modes:  $\beta_{HE}$  for even and odd  $HE_{21}$  modes;  $\beta_{TE}$  for the  $TE_{01}$  mode; and  $\beta_{TM}$  for the  $TM_{01}$  mode.

To transform the output beam from the fiber into a CVB in free-space, various conventional polarization transformation can be performed.<sup>19</sup>

The scheme of the experimental setup is presented in Figure 6. A linearly-polarized beam with wavelength  $\lambda = 532 \text{ nm}$  was diffracted onto a computer generated holographic mask and produced a set of Laguerre-Gaussian beams of various orders. Using a spatial filter we selected a  $LG_{1,0}$  beam. The beam was focused into a fiber by a  $10\times$  objective ( $O1$ ) with numerical aperture  $NA = 0.25$  and focal distance of about  $7 \text{ mm}$ . The numerical aperture of the objective matches the  $NA$  of the fiber used.

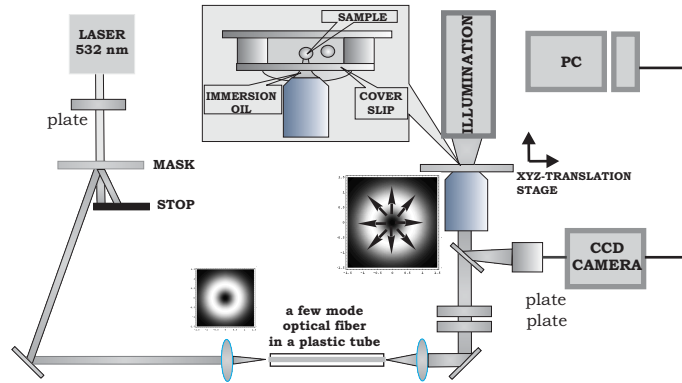


**Figure 7.** The experimental setup of the optical trap with CVB.

We put the fiber inside a plastic tube to prevent it from twisting, turning or moving.

Experimentally the presence of  $LP_{11}$  modes is denoted by a doughnut shaped intensity. To distinguish between the various modes of this group and to establish the output polarization states we used a polarization analyzer. In this case a characteristic two lobe pattern with a dark line in the middle appears. The  $TE_{01}$  and  $TM_{01}$  were distinguished from the  $HE_{21}$  modes by rotation of the analyzer.

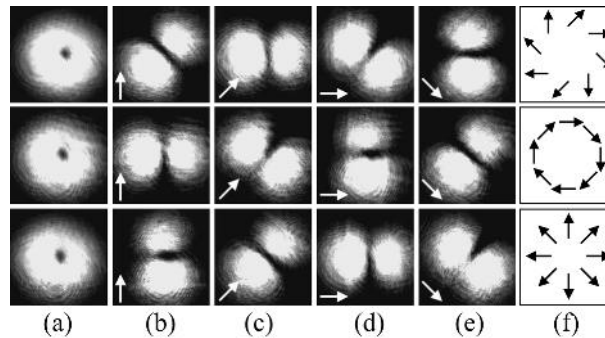


**Figure 8.** The  $+\sigma$  input polarization. In the first row, the intensity distribution of the beam that emerges from the fiber: (a) directly with no external polarizing elements, (b)-(e) after passing a analyzer orientated in the direction of the arrow. (f) depicts the polarization states deduced from the polarization measurements. In the second row, an azimuthally polarized beam, obtained from the output through a 45-degree clockwise polarization rotation. In the third row, a radially polarized beam, obtained through a 45-degree counterclockwise polarization rotation.

The first row of Figure 8 shows the output beam in the case of a  $+\sigma$  input beam. Analyzing its polarization we deduced that we had indeed excited an in-phase combination of  $TE_{01}$  and  $TM_{01}$  modes, i.e. a set of a azimuthal and radial CVB. With a two half-wave plate pure polarization rotator<sup>5,6</sup> we transformed this beam to the azimuthal (Figure 8, second row) and radial (Figure 8, third row) CVB.

The efficiency of the transformation of the incident Laguerre-Gaussian beam into a CVB was approximately 50%.

#### 4. OPTICAL TRAP WITH CVB

CVB generated with the fiber was focused by an oil-immersion microscope objective with magnification of 100 and numerical aperture of 1.3. A sample chamber mounted on a microscope stage is placed above the objective and backlit with white-light illumination. The particles are viewed through the same objective by means of a beam splitter and video camera. Video sequences were recorded with a frame-grabber.

Two low-index particle systems were studied. The first system (system *LI*) consisted of water droplets in acetophenone and was prepared following.<sup>21</sup> The second system of low-index particles (system *LII*) consisted of hollow glass spheres with radius between 2 and 15  $\mu\text{m}$  in deionized water.

A system of high-index particles (system *HI*) (G. Kisker GbR) was polystyrene beads ( $n_p = 1.59$ ) of different radii dispersed in de-ionized water.

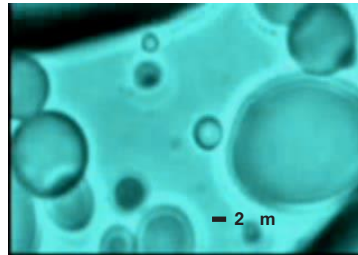


**Figure 9.** (Azimuthally polarized CVB traps a water drop in acetophenone.

Before using CVB for optical trapping we studied the behavior of three types of particles in the field of the conventional Gaussian beam focused with the same optical system. We observed that a beam of about  $3\text{mW}$  power traps the *HI* particles and repels the low-refractive index particles *LII* (hard spheres) of all sizes what we possessed (between  $1\mu$  and  $15\mu$ ). These observations fit with previously described results. The unusual result was that the gaussian beam also traps the low-refractive index particles *LI* (i.e. soft spheres). We will comment on this observation later.

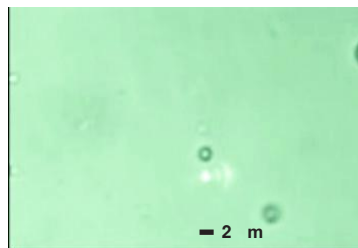


**Figure 10.** Radially polarized beam repels a hard low-index sphere and traps a high-index sphere.

Then we generated a doughnut beam with linear polarization using the same mask as one shown in Figure 7 and applied this beam for the trap. This beam traps the particles of all three systems.

After these experiments we produced the radially or azimuthally polarized CVB beams. We could not measure the intensity distribution at the focal plane of our high NA objective, where the focal spot size is less than  $1\mu$ . The image of the beam at a glass plate placed about  $20\mu$  from the focal plane showed a doughnut-shaped distribution of the intensity. With the plate placed even farther from the focal plane we saw the interference pattern resulting from the CVB and a reflected beam from the plates surface. This pattern displayed an optical vortex in the CVB.

Let us now consider the experimental results obtained using the CVB. First we observed that both the radially and azimuthally polarized CVB trapped the high-index particles *HI* and repelled the low-index particles of the

system *LII*, i.e. hard spheres with radii between 1 and 5  $\mu\text{m}$ . These results agreed with numerical results shown at Figure 2 and 3.

The unusual result was that every size of the soft spheres *LI* could be trapped by both the radially and azimuthally CVB beams.

Hence, we found out a good correspondence between the calculated and numerical results at the range of sizes between 1 and 5  $\mu\text{m}$  for hard particles. It was predicted<sup>10</sup> that the strongly focused azimuthal beam provides a stable trap for low-index particle, while the radial CVB can trap high-index particles. We showed that this is possible only for particles in the Rayleigh regime of sizes. For micron-size particles both the radially and azimuthally polarized CVB trapped the high-index particles HI and repelled the low-index particles. For stable trapping the most important condition is to produce the restoring force at the transversal direction, because in the axial direction the repelling force may be compensated by the scattering radiation force.

However, the drops of micron- and sub-micron sizes of high-index liquid dispersed in the low-index medium can be trapped by an optical beam of any profiles and polarization distribution. One of the possible explanations of this observation can be changes of the morphology of the drops by action of radiation forces. In particular in<sup>21</sup> a shrinkage of the droplets resulting from irradiance by the optical beam. Suppose that the drop changes its form in such a way that optical trapping becomes energetically favorable, this is only possible for non-rigid particles. This could explain the observed trapping of the drops independent of the incident beam profile.

## ACKNOWLEDGMENTS

We acknowledge K. Dholakia for providing us with the low-index spheres. This research was carried out in the framework of ESF/PESC (Eurocores on Sons), through grant 02-PE-SONS-063-NOMSAN, and with the financial support of the Spanish Ministry of Science and Technology.

## REFERENCES

1. D. G. Grier, "A revolution in optical manipulation," *Nature* **424**, pp. 810–816, 2003.
2. R. H. Jordan and D. G. Hall, "Free-space azimuthal paraxial wave equation: the azimuthal *bessel\_gauss* beam solution," *Optics Lett.* **19**, pp. 427–429, 1994.
3. D. G. Hall, "Vector-beam solutions of maxwell wave equation," *Optics Lett.* **21**, pp. 9–11, 1996.
4. L. E. Helseth, "Focusing of atoms with strongly confined light potentials," *Optics Commun.* **212**, pp. 343–352, 2002.
5. V. G. Niziev and A. V. Nesterov, "Influence of beam polarization on laser cutting efficiency," *J. Phys. D* **32**, pp. 1455–1461, 1999.
6. Q. Zhan and J. R. Leger, "Microellipsometer with radial symmetry," *Applied Optics* **41**, pp. 4630–4637, 2002.
7. L. Novotny, M. R. Beversluis, K. S. Youngworth, and T. G. Brown, "Longitudinal field modes probed by single molecules," *Phys. Rev. Lett.* **86**, pp. 5251–5255, 2001.
8. K. S. Youngworth and T. G. Brown, "Focusing of high numerical aperture cylindrical-vector beams," *Optics Express* **7**, pp. 77–87, 2000.
9. Q. Zhan and J. R. Leger, "Focus shaping using cylindrical vector beams," *Optics Express* **10**, pp. 324–331, 2002.
10. Q. Zhan, "Radiation forces on a dielectric sphere produced by highly focused cylindrical vector beams," *J. Opt. A: Pure Appl. Opt.* **5**, pp. 229–232, 2003.
11. T. Thusty, A. Meller, and R. Bar-Ziv, "Optical gradient forces of strongly localized fields," *Phys. Rev. Lett.* **81**, pp. 1738–1742, 1998.
12. K. T. Gahagan and J. G. A. Swartzlander, "Optical vortex trapping of particles," *Optics Lett.* **21**, pp. 827–829, 1996.
13. S. C. Tidwell, G. H. Kim, and W. D. Kimura, "Efficient radially polarized laser-beam generation with a double interferometer," *Applied Optics* **32**, pp. 5222–5229, 1993.

14. R. Oron, S. Blit, N. Davidson, A. A. Friesem, A. Bomzon, and E. Hasman, "The formation of laser beams with pure azimuthal or radial polarization," *Appl. Phys. Lett.* **77**, pp. 3322–3324, 2000.
15. Z. Bomzon, G. Biener, V. Kleiner, and E. Hasman, "Radially and azimuthally polarized beams generated by space-variant dielectric subwavelength gratings," *Optics Lett.* **27**, pp. 285–287, 2002.
16. M. Stalder and M. Schadt, "Linearly polarized light with axial symmetry generated by liquid-crystal polarization converters," *Optics Lett.* **21**, pp. 1948–1950, 1996.
17. T. Erdogan, O. King, G. W. Wicks, D. G. Hall, E. H. Anderson, and M. J. Rooks, "Circularly symmetric operation of a concentric circle-grating, surface-emitting, *algaas/gaas* quantum-well semiconductor laser," *Appl. Phys. Lett.* **60**, pp. 1921–1923, 1992.
18. T. Grosjean, D. Courjon, and M. Spajer, "An all-fiber device for generating radially and other polarized light beams," *Optics Commun.* **203**, pp. 1–5, 2002.
19. G. Volpe and D. Petrov, "Generation of cylindrical vector beams with few-mode fibers excited by laguerre-gaussian beams," *Optics Commun.* , 2004.
20. A. W. Snyder and J. D. Love, *Optical Waveguide Theory*, Chapman and Hall, London, 1983.
21. K. T. Gahagan and J. G. A. Swartzlander, "Trapping of low-index microparticles in an optical vortex," *J. Opt. Soc. Amer. B* **15**, pp. 524–534, 1998.